

Article

Application of Potassium Ion Deposition in Determining the Impact of Support Reducibility on Catalytic Activity of Au/Ceria-Zirconia Catalysts in CO Oxidation, NO Oxidation, and C₃H₈ Combustion

Ewa M. Iwanek (nee Wilczkowska)^{1,*}, Leonarda F. Liotta^{2,*} , Shazam Williams³, Linjie Hu³, Krishelle Calilung³, Giuseppe Pantaleo² , Zbigniew Kaszukur⁴ , Donald W. Kirk⁵  and Marek Gliński⁶

¹ Faculty of Applied Science and Technology, Sheridan College, Brampton, ON L6Y5H9, Canada

² Istituto per lo Studio di Materiali Nanostrutturati (ISMN)-CNR, I-90146 Palermo, Italy; giuseppe-pantaleo@cnr.it

³ DCL International Inc., Concord, ON L4K 4T5, Canada; swilliams@dcl-inc.com (S.W.); rhu@dcl-inc.com (L.H.); KCalilung@dcl-inc.com (K.C.)

⁴ Institute of Physical Chemistry, Polish Academy of Sciences, 01-224 Warsaw, Poland; zkaszkur@ichf.edu.pl

⁵ Department of Chemical Engineering and Applied Science, University of Toronto, Toronto, ON M5S3E5, Canada; don.kirk@utoronto.ca

⁶ Faculty of Chemistry, Warsaw University of Technology, 00-664 Warsaw, Poland; marekg@ch.pw.edu.pl

* Correspondence: ewa.iwanek@sheridancollege.ca (E.M.I.); leonardafrancesca.liotta@cnr.it (L.F.L.)

Received: 25 May 2020; Accepted: 17 June 2020; Published: 19 June 2020



Abstract: The purpose of the study was to show how a controlled, subtle change of the reducibility of the support by deposition of potassium ions impacts the activity of gold catalysts. Since the activity of supported gold catalysts in carbon monoxide oxidation is known to strongly depend on the reducibility of the support, this reaction was chosen as the model reaction. The results of tests conducted in a simple system in which the only reagents were CO and O₂ showed good agreement with the CO activity trend in tests performed in a complex stream of reagents, which also contained CH₄, C₂H₆, C₃H₈, NO, and water vapor. The results of the X-ray Diffraction (XRD) studies revealed that the support has the composition Ce_{0.85}Zr_{0.15}O₂, that its lattice constant is the same for all samples, and that gold is mostly present in the metallic phase. The reducibility of the systems was established based on Temperature Programmed Reduction (TPR) and in situ XRD measurements in H₂ atmosphere. The results show that the low temperature reduction peak, which is due to the presence of gold, is shifted to a higher value by the presence of 0.3 at% potassium ions on the surface. Moreover, the increase of the potassium loading leads to a more pronounced shift. The T₅₀ of CO oxidation in the simple model stream was found to exhibit an excellent linear correlation with the maximum temperature of the low temperature reduction peak of Au catalysts. This means that stabilizing oxygen with a known amount of potassium ions can be numerically used to estimate the T₅₀ in CO oxidation. The results in the complex stream also showed a similar dependence of CO conversion on reducibility, though there was no substantial difference in the activity of the catalysts in other reactions regardless of the potassium loading. These studies have shown that the influence of potassium varies depending on the reaction, which highlights differences in the impact of reducibility and importance of other factors in these reactions.

Keywords: CO oxidation; potassium poisoning; gold nanoparticles; ceria-zirconia; NO oxidation; propane combustion

1. Introduction

Due to the fact that supported gold catalysts exhibit well-documented high activity in low temperature CO oxidation [1–4] they are commonly studied for automotive applications, despite the fact that the platinum, palladium, and ruthenium catalysts are highly active in the combustion of hydrocarbons [5]. It has been shown that there is a substantial influence of the support, gold precursor, and the method of synthesis on the activity of the resulting catalytic system [6]. Since the reducibility of the support is a key factor in CO oxidation this reaction was selected as the model reaction, but additional testing in a stream whose composition simulated the lean-burn natural gas engine exhaust has also been performed. The sensitivity of gold catalyst activity to changes in support reducibility means that non-stoichiometric oxides such as ceria and cerium-zirconium mixed oxides are commonly used as supports. However, the change of the support composition has a substantial impact not only on the reducibility of the system, but also on variables such as: lattice parameter of the support and hence the interaction of gold with the support, etc. This is why the goal of this study was to prepare a specific fraction of one batch of the calcined support with a specific composition, onto which first gold was deposited, followed by the deposition of potassium ions, so that the obtained systems would differ mainly in the potassium loading.

Potassium carbonate has been used in the gasification of coal for decades [7–9]. Its activity is attributed to the mobility of the potassium ions [7]. Studies of a Cu-V-K-Cl/TiO₂ catalyst by Ciambelli et al. have shown that the catalyst “is able to strongly lower the ignition temperature of different carbon materials, from fullerene to graphite, to carbon particulate from diesel engine and from oil fired power plants” [10] and the activity of such catalysts in soot oxidation was observed to depend on the reducibility of the system [11]. The addition of potassium ions on ceria [12] or ceria-zirconia [13] has also been successfully applied in diesel soot catalysts. Upon comparison of the activity of alkali and alkaline earth metal oxides in soot combustion [14] it was concluded that alkaline earth metals are worse catalysts due to a lower mobility of the surface species, which is in line with the reports on coal gasification [8]. In the current work, potassium carbonate was deposited onto the surface of gold catalysts supported on ceria-zirconia as a novel method of testing how the suppression of the reducibility of the support influences the activity of the catalytic system in CO oxidation and other reactions in a multicomponent stream.

Currently, research in gold catalysts is carried out in the hope to keep the superior activity in CO oxidation while increasing the activity in the oxidation of VOCs. Therefore, tests were carried out in a multicomponent stream which included CO, saturated hydrocarbons, water vapor, NO, CO₂, and nitrogen and the gas flow rate and volume of the catalyst bed (gas hourly space velocity, GHSV) was similar to normal reaction conditions in a catalytic converter. Among volatile organic compounds propene is very commonly studied in research on gold catalysts [15–17]. The results indicate that the complete combustion of propene can take place at temperatures above 200 °C [3]. As shown by comparative studies of propane and propene combustion, the combustion of saturated hydrocarbons is relatively more difficult than that of unsaturated ones [3,6]. This is why propane was used in our tests. Complete oxidation of propane on nano-gold catalysts supported on ceria, zirconia, and ceria-rich ceria-zirconia was studied by Ali et al. [18]. The activity tests were carried out in a stream which contained only propane (0.5 vol%) in helium. Their results show that the performance of Au/CeO₂ was superior to that of Au/ZrO₂. The activity of Au supported on the ceria doped with zirconium ions was an intermediate between those of gold on each of the two pure supports. However, the two pure oxides and the mixed oxide have different structures and properties, so a meaningful comparison which could contribute to the understanding of how reducibility of the support is not possible with these systems. Therefore, the focus of our study was one kind of support, Ce_{0.85}Zr_{0.15}O₂, which came from the same batch and the large, 150–250 μm, fraction was used for catalyst preparation. The differences between the support in each of the samples are negligible and hence the differences in reducibility can be attributed to the species deposited onto the surface of these particles (gold, potassium, or both) and their interaction with the support.

2. Results

X-ray Diffraction patterns of the Au catalysts without and with 0.3 and 0.6 at% potassium ions, respectively, are shown in Figure 1 along with that of the ceria-zirconia doped with 0.3 at% potassium ions. They show that the main phase present in these systems is the ceria-zirconia solid solution with the fluorite type structure. The values of the lattice constant of the support for these four samples were comparable within the experimental error (Table 1). The strain of the support lattice is small in the case of all samples (Table 1). The Ce:Zr ratio determined using XRD was 85:15, which is in accordance with the nominal composition of the cerium-zirconium mixed oxide. No signals from a potassium-containing phase have been detected in the XRD patterns. The Au catalysts contain a slightly visible Au (111) peak at a scattering angle of approximately 38.2° that was used to estimate the size of the gold nanoparticles. They are approximately 4 nm in diameter. The gold loading was equal to 0.2 at% (1 wt%) for all catalysts and the potassium concentration corresponds to 0.3 and 0.6 at%, respectively, as determined by the ICP analysis. The specific surface area values of the samples were between 70–75 m²/g, regardless of the presence of Au and K.

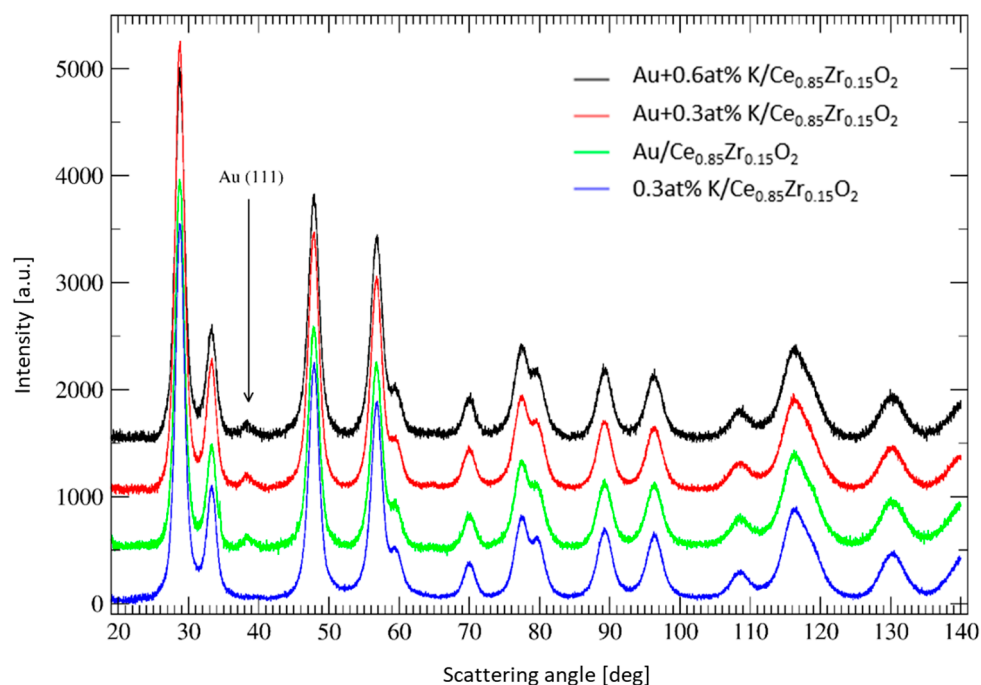


Figure 1. X-ray Diffraction patterns of Au/Ce_{0.85}Zr_{0.15}O₂ and Au + K (0.3 and 0.6 at%)/Ce_{0.85}Zr_{0.15}O₂ catalysts and the support doped with 0.3 at% potassium.

Table 1. Results of X-ray Diffraction studies: Support lattice parameter, strain of support lattice, average particle size of support and gold in catalysts, and the potassium-doped support; the regression error of the last figure is shown in parentheses.

	Support Lattice Constant [Å]	Strain of Support Lattice [-]	Support Particle Size [nm]	Au Particle Size [nm]
Au/Ce _{0.85} Zr _{0.15} O ₂	5.3728(7)	0.007(2)	5.2(9)	4(1)
Au + 0.3at% K/Ce _{0.85} Zr _{0.15} O ₂	5.3729(8)	0.005(1)	4.6(5)	4(1)
Au + 0.6at% K/Ce _{0.85} Zr _{0.15} O ₂	5.3736(8)	0.003(1)	4.2(3)	4(1)
0.3at% K/Ce _{0.85} Zr _{0.15} O ₂	5.3737(6)	0.003(1)	4.4(3)	n.d.

The SEM results revealed no substantial differences in the topographies of the samples (Figure 2A–D). The SEM-EDX for the catalyst with 0.6 at% potassium ions can be seen in Figure 2E.

Visible signals from all components can be seen, including a pronounced potassium signal. The Zr/(Zr + Ce) ratio is 17 at%, which is much closer to the value obtained from XRD than those obtained by XPS (Table 2). Hence, to sum up this portion of results, it can be stated that there are no substantial differences between the topography of the catalysts and their composition (other than the potassium ion content), which enables meaningful comparisons and analysis of activity results.

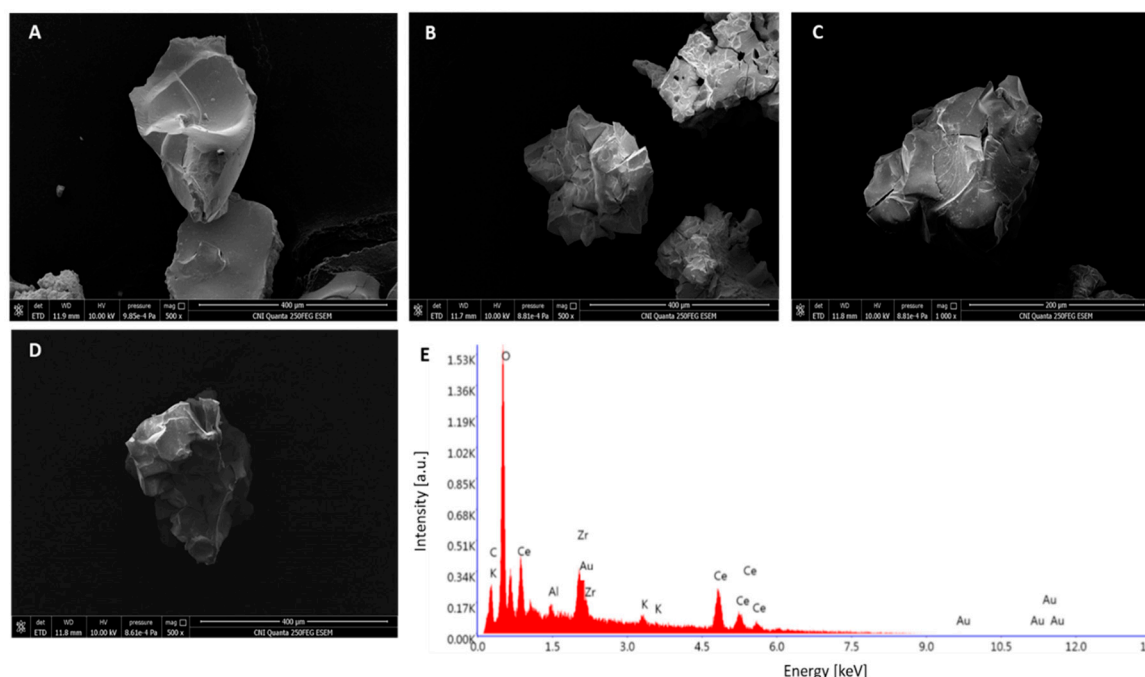


Figure 2. SEM-EDX results: Images of the gold containing catalysts without (A) and with potassium: 0.3 (B) and 0.6 at% (C), and the support with 0.3 at% potassium ions (D), as well as the EDX results for Au + 0.6 at% K/Ce_{0.85}Zr_{0.15}O₂.

Table 2. Results of X-ray Photoelectron Spectroscopy studies.

	Au /Support	Au + 0.3at% K/Support	Au + 0.6at% K/Support	0.3 at% K/Support
Zr/(Zr + Ce) [%]	21–25	21–26	22–25	22–26
Au 4f [at%]	2.8–4.1	3.0–3.9	2.9–4.2	n.d.
K 2p [at%]	n.d.	0.8–2.0	2.8–3.9	0.6–2.1
Au 4f components [%]				
Au ⁰	88 ± 4	85 ± 6	86 ± 4	N/A
Au ⁺	9 ± 2	10 ± 3	10 ± 2	N/A
Au ³⁺	3 ± 1	5 ± 2	4 ± 1	N/A

X-ray Photoelectron Spectroscopy measurements were conducted on at least four spots of each catalyst due to the possibility of surface inhomogeneity and hence ranges are given in Table 2. The XPS results have shown that all of the catalysts had only the elements which they were designed to have. Signals from all of them are visible in the survey spectra (not shown). The amount of zirconium on the surface is higher than the value found using XRD (Table 2). This is in agreement with previous findings about Zr enrichment occurring in ceria-zirconia solutions after thermal treatment at high temperature [19]. Moreover, the gold and potassium loadings were also higher than those determined by ICP, which was expected due to the fact they were deposited onto the support after support synthesis. The reason for using this method of catalyst preparation was to have all the catalysts made with the 150–250 μm fraction of the support onto which gold and potassium carbonate were deposited

in sequence without changing the bulk properties. Hence, comparisons made with the potassium ion loaded support are valid.

The Au surface content as determined by XPS seems unaffected by the presence of K and the same conclusion can be drawn for K surface concentration (Table 2). These experiments revealed heterogeneity of the surface in terms of both the gold and potassium distribution. However, in several of the tested spots of the Au + 0.6 at% K/Ce_{0.85}Zr_{0.15}O₂ catalyst an Au:K ratio very close to 1:1 has been observed. This may indicate a formation of a compound with such stoichiometry, e.g., aurate or an alloy. Nevertheless, a carbonate signal in the C 1s detailed regions suggests that at least a part of the potassium is in the form of the carbonate, although the phase was not detected by XRD.

The Au 4f detailed regions of the XPS spectra collected for the catalysts are presented in Figure 3. The Au 4f peaks were fitted with three doublets with a spin orbital splitting of 3.7 eV. The Au 4f_{7/2} components were located at the binding energy of 84.0, 85.0, and 86.0 eV (Figure 3), which corresponded to Au⁰, Au⁺, and Au³⁺, respectively, although there are some discrepancies in the literature regarding the position of the binding energy of the Au³⁺ component [20,21]. The distribution of Au shows that the majority of the gold is found in the metallic form (Table 2), which is in line with the results of the XRD measurements. This can be expected considering the relatively high calcination temperature. Usually, the calcination treatment reduces ionic gold species to the metallic state [22]. The reason why the calcination of the catalysts was carried out at 550 °C is that the catalytic tests were to be performed up to that temperature. Therefore, such a calcination procedure ensures that the analysis of the catalytic tests is not obscured by additional sintering of the support.

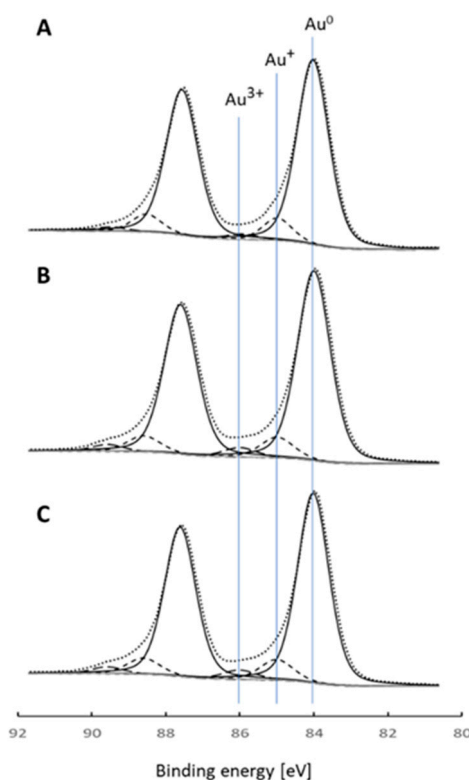


Figure 3. XPS results for Au 4f detailed regions of the catalysts: (A) Au/Ce_{0.85}Zr_{0.15}O₂, (B) Au + 0.3 at%K/Ce_{0.85}Zr_{0.15}O₂, and (C) Au + 0.6 at%K/Ce_{0.85}Zr_{0.15}O₂.

The Temperature Programmed Reduction profiles obtained for the investigated systems are depicted in Figure 4A. The reduction of the potassium doped support (yellow curve) is characterized by a main peak with maximum at 515 °C that is preceded by a shoulder at 380 °C and followed by a broad signal at 760 °C. A similar profile was registered for the potassium-free ceria-zirconia (red

curve) and it is in agreement with the typical reduction of cerium-zirconium oxides, the number and position of reduction peaks depending on the exact composition and oxygen mobility of the solid solutions [23,24]. For the potassium-doped support, the hydrogen consumption of the main peak is centered at 515 °C and it corresponds to $24 \text{ mL} \cdot \text{g}_{\text{CeZr}}^{-1}$, while the broad feature at 760 °C corresponds to $10 \text{ mL} \cdot \text{g}_{\text{CeZr}}^{-1}$. Within the experimental error ($\pm 10\%$) no differences were observed for the hydrogen consumption values associated with the TPR curve of the potassium-free ceria-zirconia. Such values corresponding to an overall hydrogen consumption of $34 \text{ mL} \cdot \text{g}_{\text{CeZr}}^{-1}$, or $38.3 \text{ mL} \cdot \text{g}_{\text{CeO}_2}^{-1}$ are in good agreement with values ranging between 40–50 $\text{mL} \cdot \text{g}_{\text{CeO}_2}^{-1}$ previously observed for samples with composition $\text{Ce}_{0.6}\text{Zr}_{0.4}\text{O}_2$ and improved oxygen mobility [23].

The presence of gold results in a low temperature reduction peak, between 100–140 °C, that is due to the shift of the main peaks at 515 °C detected for the CeZr supports (with and without potassium). That peak is followed by the same very broad signal of hydrogen uptake at 760 °C, common to the supports. TPR curves with similar features are typical for ceria and cerium-zirconium mixed oxides doped with Au [25,26], as well as Pt [27] and Pd [28]. According to the literature [25–28] the noble metal increases the oxygen mobility of the part of ceria or ceria-zirconia where the metallic nanoparticles are well dispersed, leaving the part with low oxygen mobility unaffected and reducible at around 800 °C. The influence of the potassium loading can be seen as shifting the maximum of the low temperature reduction signal to slightly higher values. For the Au/support system the maximum of the reduction occurs at 101 °C. In the systems with potassium the maximum takes place at 113 and 138 °C, for the 0.3 at% and 0.6% K loading, respectively.

The increased reducibility of the Au/ceria-zirconia catalysts (with and without K), associated with the low-temperature peak between 100–140 °C, implies, according to the literature [25], hydrogen activation on the Au metal nanoparticles and subsequent spillover on the support, with promotion of the reduction at low temperature. It is evident that increasing K loading from 0.3 to 0.6 at% inhibits such a spillover effect with a consequent shift of the maximum of the low temperature reduction peak to slightly higher values. Based on this it can be supposed that Au nanoparticles and K ions are in close contact. Together with a 1:1 ratio of Au:K in some of the spots of the Au + 0.6 at% K/ $\text{Ce}_{0.85}\text{Zr}_{0.15}\text{O}_2$ catalyst in the XPS measurement, it may be indicative of the formation of a compound or another type of interaction, which is why the difference of T_{max} of the low-temperature reduction signal of Au/ $\text{Ce}_{0.85}\text{Zr}_{0.15}\text{O}_2$ and Au + 0.6 at% K/ $\text{Ce}_{0.85}\text{Zr}_{0.15}\text{O}_2$ is larger than twice the difference between Au/ $\text{Ce}_{0.85}\text{Zr}_{0.15}\text{O}_2$ and Au + 0.3 at% K/ $\text{Ce}_{0.85}\text{Zr}_{0.15}\text{O}_2$. However, it should be kept in mind that this ratio was only observed with the most surface-sensitive technique and that an enrichment in Au with the increase of probing depth was shown by EDX.

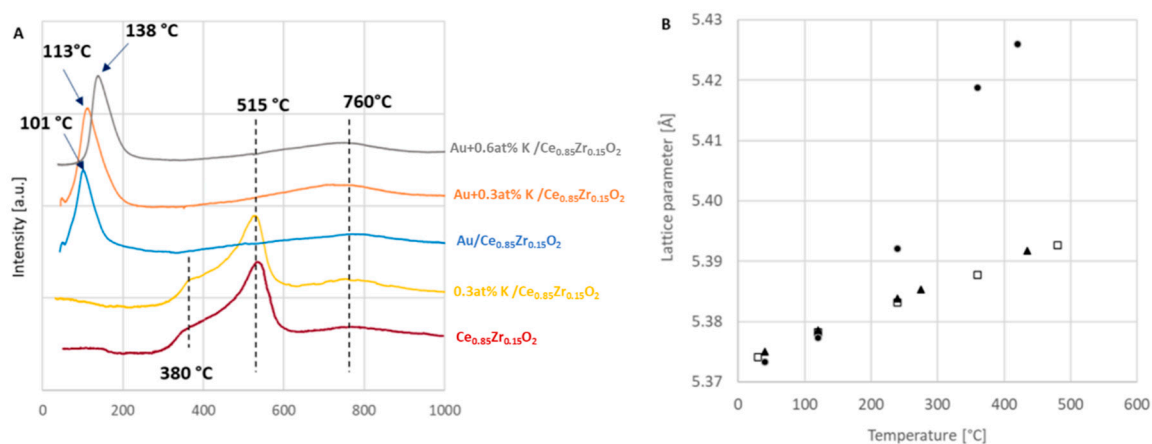


Figure 4. Results of (A) Temperature Programmed Reduction experiments and (B) in situ X-ray Diffraction studies of the Au + 0.3 at% K/support system in three different atmospheres: H₂ (spheres), O₂ (squares), and He (triangles).

The overall hydrogen consumption registered for the three Au supported catalysts was unaffected by the K presence, at the two atomic concentrations herein used, with total values around 34–37 mL·g_{CeZr}⁻¹ and the hydrogen consumed at around 760 °C being the same for all three samples and equal to 10 mL g_{CeZr}⁻¹.

Another way to study reduction is by the application of in situ X-ray Diffraction studies in hydrogen. The information acquired from such a measurement can easily differentiate between a small surface reduction and a substantial reduction by the extent of the change in the lattice parameter of the support. The tests were conducted in three atmospheres: hydrogen, helium, and oxygen. The aim was to investigate how the interaction of gold with the support changes the reduction behavior of the catalysts and to see if the influence of the presence of potassium can be observed, as in the case of the TPR measurements. The results of X-ray Diffraction studies carried out on the gold catalyst with 0.3 at% potassium are shown in Figure 4B. The squares correspond to measurements carried out in oxygen and the triangles to those performed in helium. These two sets of points fall on one line, which corresponds to thermal expansion of the support lattice. The difference between the value noted at the lowest temperature and 480 °C is 0.018 Å. In contrast, in the results obtained during treatment with hydrogen it can be seen that only at the two lower temperatures, i.e., 40 and 120 °C, the results are the same as those measured in the other two atmospheres, but the third value is substantially higher than the corresponding values of the support lattice parameter in He and O₂. The two values obtained at the two highest temperatures, namely 360 and 420 °C, are even further away from the values typical for thermal expansion. The support lattice parameter at the highest temperature with hydrogen is 0.034 Å higher than those in the oxygen and in helium. Therefore, the reduction of the catalysts is not a superficial one, but a structural change occurs. Similar results have been noted for the catalyst with the higher potassium loading. Since this reduction is already visible at temperatures around 240 °C, which is much below the temperature at which the support + 0.3 at% K releases its oxygen, these results indicate that this substantial reduction is facilitated by the presence of gold. In situ XRD studies in hydrogen performed by Bekheet et al. have also shown pronounced changes in the ceria lattice parameter and the lattice parameter of Sm-doped ceria [29]. That study found no CeH_x phase, but instead the formation of ordered oxygen vacancies and changes of both the stoichiometry and crystallographic system for pure CeO_x, whereas the Sm stabilized the structure and no transition to a rhombohedral phase despite the change of the stoichiometry. A similar situation of a substantial support lattice parameter change without a phase change was noted by us for the ceria-zirconia lattice. Investigation of the lattice parameter of cerium-zirconium mixed oxides has been conducted by some of us in a CO/He mixture [30].

At all temperatures the activity in CO oxidation of the gold catalyst without potassium was the highest in both the multicomponent stream and the stream with only 1 vol% CO and 1 vol% O₂ in helium (Figure 5A,B, respectively), whereas the activity of the potassium-doped support is negligible up to the temperature of approximately 350 °C. In Figure 5B the dotted lines represent extrapolation of the curves up to 100% of conversion not registered in our experimental conditions.

The comparison of the two sets of results clearly shows the negative impact of the presence of other inlet stream components in the feed on the CO conversion. Presumably, the most pronounced effect is that of the high content of water vapor, as the presence of water has been shown to inhibit CO oxidation [31]. The activity of the catalyst with 0.3 at% potassium was lower than that of Au/Ce_{0.85}Zr_{0.15}O₂ in the whole range of studied temperatures. The activity of the catalyst with 0.6 at% potassium was consistently lower than that of the catalyst with 0.3 at%. This indicates that the increase of potassium loading further hinders the reducibility of the support, which is responsible for activity in CO oxidation in accordance with the Mars-van Krevelen mechanism [4] and, as we have demonstrated, from the linear relationship between the reducibility of Au/ceria catalysts and CO oxidation activity [25]. This agrees with our TPR results, which have shown that the addition of 0.3 and 0.6 at% potassium shift the low temperature reduction peak to higher temperatures. In fact, a linear dependence with

excellent correlation between the T_{50} determined in the tests with 1 vol% CO, 1 vol% O₂, balance He, and the T_{max} of the reduction peak was found (Figure 6).

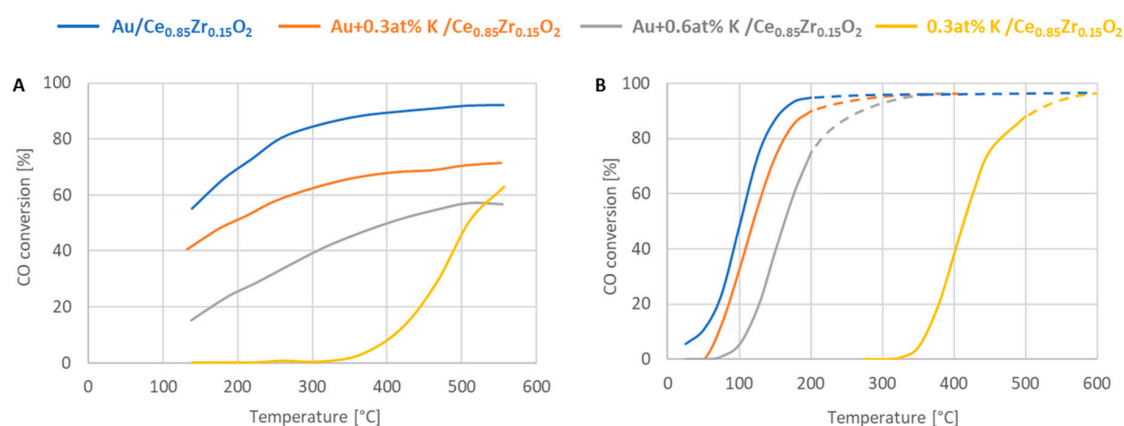


Figure 5. Conversion of carbon monoxide in (A) activity tests in the multicomponent stream and (B) the stream with 1 vol% CO + 1 vol% O₂ in He, on the gold catalysts and potassium-doped support.

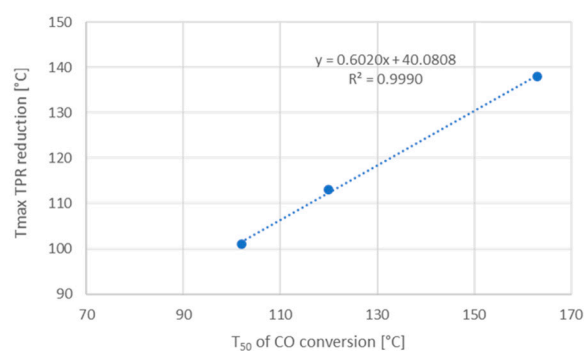


Figure 6. Correlation between T_{max} reduction in TPR curves and T_{50} of CO conversion in a stream containing 1 vol% CO + 1 vol% O₂ in He.

The activity of these systems in the propane combustion and NO oxidation are summed up in Figure 7. It is noteworthy that the results of the activity tests revealed that under the studied conditions the gold catalysts are not superior to the potassium-doped support in propane oxidation, i.e., their activity is comparable in the studied range of temperatures (Figure 7A). Both systems with potassium, i.e., with and without gold, exhibited the same activity. When interpreting this in the light of the results of our TPR and in situ XRD studies, it can be stated that the interaction of gold and the support does not impact the activity of the system in this reaction. The only catalyst with a substantially lower activity in propane combustion is the catalyst with 0.6 at% potassium ions deposited onto its surface. In contrast to both CO oxidation and propane combustion, the conversion of NO to NO₂ at temperatures up to 550 °C is the highest on the potassium-doped support. Figure 7B shows the NO₂/NO ratio in the outlet streams. The effect of potassium on the activity of gold catalysts in this reaction is visible, but changes in the studied temperature range: at temperatures up to 265 °C the Au + 0.6 at%/Ce_{0.85}Zr_{0.15}O₂ system exhibits the highest activity and Au/Ce_{0.85}Zr_{0.15}O₂ has the lowest activity, whereas in the range 418–509 °C the Au + 0.6 at%/Ce_{0.85}Zr_{0.15}O₂ exhibits the highest activity in NO oxidation (Figure 7B). At the highest studied temperature, the activity of the potassium-doped support and the gold-containing systems are all similar.

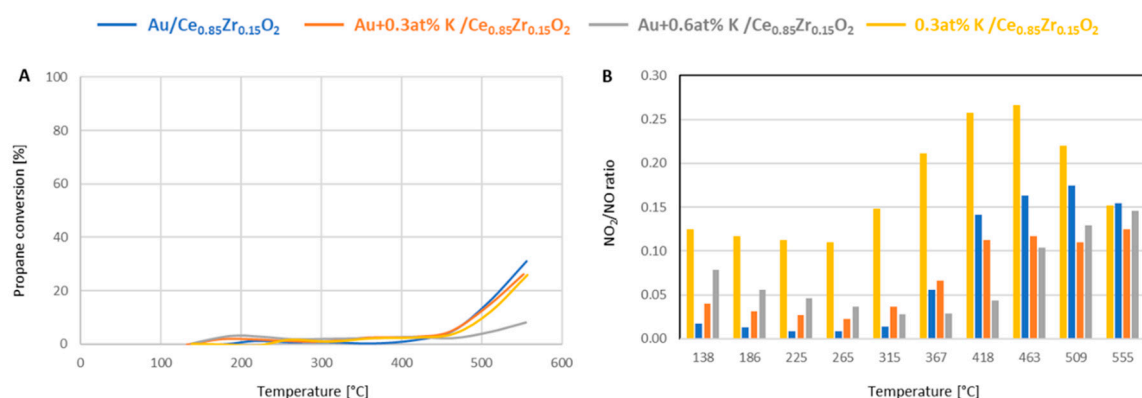


Figure 7. Activity test results: (A) Conversion of propane and (B) NO₂/NO ratio in the outlet stream for the gold catalysts and potassium-doped support.

3. Materials and Methods

The catalysts were prepared from ceria-zirconia which was obtained via the aqueous route from ammonium ceric nitrate (analytical grade, BDH, Randor, PA, USA) and zirconyl nitrate (analytical grade, Fisher, Ottawa, ON, Canada). The mixture of 26.63 g of zirconyl nitrate and 48.42 g of ammonium ceric nitrate was dissolved in 100 mL of water and a concentrated ammonium hydroxide solution was slowly added (analytical grade, Caledon, Georgetown, ON, Canada). The solid was filtered, dried, calcined at 550 °C for 4 h, and crushed. The 150–250 μm fraction was divided into four parts and three of them were placed in a beaker containing an appropriate volume of a solution of HAuCl₄·H₂O (0.01 mol·L⁻¹) (analytical grade, Sigma-Aldrich, Oakville, ON, Canada) in order to prepare catalysts with Au loading equal to 1 wt%. The pH value of the suspension was adjusted to 8.5 with a potassium carbonate solution (0.5 mol·L⁻¹) and the mixture was stirred overnight at 65 °C. The precipitate was washed several times until the pH of the filtrate was neutral and the test with AgNO₃ came out negative. The material was calcined at 350 °C for 3 h and divided into three parts (6 g each). Two of them were dosed with a potassium carbonate solution (analytical grade, Fisher, Ottawa, ON, Canada), 0.750 and 1.50 mL, respectively, so as to obtain catalysts with a final potassium ion loading of 0.3 and 0.6 at%. All three catalysts were then calcined at 550 °C for 4 h. The support also underwent the same thermal treatment as the others and was then dosed with the solution of potassium carbonate to a final loading of 0.3 at%.

Two sets of activity tests were carried out. Both were performed in tubular flow-through reactors using 0.5 g of the catalyst. The first were performed with a gas flow rate of 1.5 L min⁻¹ in the temperature range 110–600 °C. The inlet stream contained a mixture of hydrocarbons (1000 ppm CH₄, 150 ppm C₂H₆, and 50 ppm C₃H₈), 200 ppm NO, 1000 ppm CO, 7% water vapor, 5% CO₂, 10% O₂, and balance N₂. The outlet stream composition was monitored using a MultiGas 2030 FTIR Continuous Gas Analyzer, MKS Instruments Inc. (Rochester, NY, USA). The second set of activity tests was conducted in a stream containing 1 vol% CO + 1 vol% O₂ in He (50 mL·min⁻¹).

Inductively Coupled Plasma measurements were performed using an Optima 7000 Inductively Coupled Plasma Optical Emission Spectrometer (Perkin-Elmer Inc., Waltham, MA, USA). They were used to determine the amount of gold and potassium ions present in the solutions of the samples obtained from digesting 0.3 g in sulfuric acid and then in aqua regia. The concentrations were determined using external standard calibration curves.

The specific surface area of the catalysts and potassium doped support were determined using a Micromeritics ASAP 2010 instrument (Micromeritics Instrument Corp., Norcross, GA, USA). Nitrogen physisorption was performed at 77 K. The standard pressure used was in the p/p₀ range of 0.01–0.50. The samples (approx. 0.4 g) were outgassed for 30 min at 150 °C under a vacuum prior to the

measurement. The Brunauer-Emmet-Teller equation was used to calculate the specific surface area of the samples.

The Secondary Emission Microscopy-Energy Dispersive X-ray Spectroscopy (SEM-EDX) experiments were performed on a Quanta FEG 250 instrument (Field Electron and Ion Company, FEI, Hillsboro, OR, USA). The working distance was 10 mm. Images were taken at magnifications of 500, 1000, as well as 10,000 (for EDX analysis). EDX measurements were carried out for three spots (spot size 4) of each sample using the beam energy of 10 kV.

Reduction properties of the gold catalysts and the ceria-zirconia mixed oxide were studied by Temperature Programmed Reduction (TPR) measurements. Experiments were carried out with a Micromeritics Autochem 2910 apparatus equipped with a thermal conductivity detector (TCD) (Micromeritics Instrument Corp., Norcross, GA, USA). Before starting the analyses, the catalyst (ca. 100 mg) was pretreated in a flow of 5% vol O₂ in He gas mixture (30 mL·min⁻¹) at 150 °C (10 °C min⁻¹) for 10 min to clean the surface and then cooling down in a flow of He (30 mL·min⁻¹) up to room temperature. A 5 vol% H₂ in Ar gas mixture (30 mL·min⁻¹) was used to reduce the sample by heating from room temperature to 1050 °C at the rate of 10 °C min⁻¹. The hydrogen consumption values associated with the TPR profile were determined by applying a calibration curve to the TCD signals and are quoted with a precision of ±10%.

X-ray Diffraction studies were carried out with a D5000 horizontal goniometer (Bruker AXS GmbH, Karlsruhe, Germany) equipped with a Cu anode sealed tube (K α radiation $\lambda = 1.5418 \text{ \AA}$) which operated at 40 kV, 40 mA, using Bragg-Brentano divergent beam optics with a K β filter and a LynxEye strip detector. Approximately 50 mg of the sample was smeared over the surface of porous glass, mounted to the measurement environmental chamber, exposed to oxygen (5.0 purity, flow 20 mL·min⁻¹), and measured in a sequence of rising temperatures up to approx. 420 °C, then exposed to helium (5.6 purity, flow 20 mL·min⁻¹) and measured in a sequence of temperatures down to 40 °C. Next, it was exposed to hydrogen (5.0 purity, flow 20 mL·min⁻¹) and measured in a sequence of temperatures rising to approx. 420 °C, then flushed with helium and cooled down. Each XRD measurement encompassed the range of 20–140° of scattering angle and lasted 106 min. The analysis involved averaging of several datasets, background subtraction, and fitting of the measured peaks with doublets of Voigt functions (K $\alpha_{1,2}$) (program Fityk v.1.3.0). The support peak parameters were analyzed via the Williamson-Hall plot, lattice parameter extrapolation using Nelson-Riley function and Debye-Waller factor determination. The following parameters were calculated: volume weighted average of atomic rows length D (interpreted as a support crystal size), support microstrain parameter ϵ corresponding to a range of local variations of the support lattice parameter (resulting in additional peak broadening rising with angle as $2\theta^\circ$ and the ceria-zirconia lattice parameter, as well as the average gold particle size and the Ce:Zr ratio.

The X-ray Photoelectron Spectroscopy measurements were carried out on a K-Alpha instrument (Thermo Scientific, Waltham, MA, USA). Survey spectra were obtained with a pass energy of 200 eV, 1 eV step and detailed regions, i.e., C 1s + K 2p, Au 4f, Ce 3d, Zr 3d, and O 1s were collected with a pass energy of 50 eV, 0.1 eV step. Each sample was measured at least four times and the values were averaged. The quantitative analysis of the spectra was performed after background subtraction and calibration using the C 1s signal. For quantification the K 2p doublet was fitted with a single pair of curves with a spin orbital splitting of $2.8 \pm 0.1 \text{ eV}$.

4. Conclusions

The doping of gold catalysts with potassium ions was applied to investigate the extent of stabilizing oxygen species of the support, i.e., decreasing its reducibility, and the effect on the loss of activity in CO oxidation, where support reducibility plays a crucial role. In CO oxidation in a stream containing 1 vol% CO, 1 vol% O₂, balance He, the catalyst without potassium showed superior activity. The presence of 0.3 at% potassium lowered the activity of the gold catalyst in CO oxidation and a further increase of the potassium loading led to a further drop of activity. This corresponds to the shift

of the low-temperature reduction peak in the TPR results to higher temperatures in the presence of potassium. The T_{50} is linearly correlated with the T_{max} of the reduction peak with an $R^2 = 0.999$. The reducibility of the catalysts was also probed with in situ XRD measurements which were carried out in a stream of hydrogen in the temperature range 30–400 °C. The results substantially differed than those obtained from in situ XRD tests performed in an oxygen-containing atmosphere, as well as in helium, which have shown that the crystal lattice of the support only undergoes thermal expansion in the studied temperature range in either He and O₂. In contrast, the results of the measurements carried out in a hydrogen stream have revealed a substantial change of the support lattice constant upon heating, which shows that the effect of hydrogen consumption observed in the TPR profiles is not just a matter of interaction of hydrogen with the surface oxygen of the solid.

Moreover, a similar trend for CO activity was determined in experiments in which the inlet stream contained other components, such as water vapor, NO, propane, etc., which simulated typical lean-burn automotive exhaust gases. The activity of the catalysts in propane combustion was very low and those at the highest tested temperatures showed that the presence of 1.0 wt% of gold did not have a pronounced effect on the activity. The catalyst with 0.6 at% of potassium exhibited the lowest activity in the combustion of propane. In contrast, at the highest studied temperature all three gold-containing systems exhibited the same activity in NO oxidation, regardless of the potassium loading. This strongly indicates that support reducibility is the main determining factor of activity only for CO oxidation, whereas neither the pronounced increase in reducibility due to the presence of gold nor the suppression of it due to the deposition of potassium ions plays a substantial role in the other reactions.

Author Contributions: Conceptualization, E.M.I., L.F.L., S.W., and L.H.; formal analysis, Z.K., L.F.L., G.P., and E.M.I.; investigation, L.F.L., G.P., E.M.I., L.H., and K.C.; resources, D.W.K., E.M.I., and M.G.; data curation, E.M.I., Z.K., L.F.L., and G.P.; writing—original draft preparation, E.M.I.; writing—review and editing, L.F.L., G.P., D.W.K., L.H., S.W., and M.G.; visualization, E.M.I. and Z.K.; project administration, E.M.I., J.L.H., and L.F.L.; funding acquisition, E.M.I., S.W., and D.W.K. All authors have read and agreed to the published version of the manuscript.

Funding: This research was funded by the Natural Sciences and Engineering Research Council of Canada, grant number 523834-18.

Acknowledgments: We would also like to thank Ilya Gourvich from the Centre for Nanostructure Imaging (CNI) at the University of Toronto for performing the SEM-EDX measurements, as well as the Ontario Centre for the Characterization of Advanced Materials (OCCAM) for enabling us to perform the X-ray Photoelectron Spectroscopy measurements.

Conflicts of Interest: The authors declare no conflict of interest.

References

1. Waters, R.D.; Weimer, J.J.; Smith, J.E. An investigation of the activity of coprecipitated gold catalysts for methane oxidation. *Catal. Lett.* **1995**, *30*, 181–188. [[CrossRef](#)]
2. Haruta, M. Preparation and environmental applications of supported gold catalysts. *Now Future* **1992**, *7*, 13–20.
3. Gąsior, M.; Grzybowska, B.; Samson, K.; Ruszel, M.; Haber, J. Oxidation of CO and C₃ hydrocarbons on gold dispersed on oxide supports. *Catal. Today* **2004**, *91–92*, 131–135. [[CrossRef](#)]
4. Scirè, S.; Liotta, L.F. Supported gold catalysts for the total oxidation of volatile organic compounds. *Appl. Catal. B* **2012**, *125*, 222–246. [[CrossRef](#)]
5. Liotta, L.F. Catalytic oxidation of volatile organic compounds on supported noble metals. *Appl. Catal. B* **2010**, *100*, 403–412. [[CrossRef](#)]
6. Gluhoi, A.C.; Nieuwenhuys, B.E. Catalytic oxidation of saturated hydrocarbons on multicomponent Au/Al₂O₃ catalysts. Effect of various promoters. *Catal. Today* **2007**, *119*, 305–310. [[CrossRef](#)]
7. Wigmans, T.; Elfring, R.; Moulijn, J.A. On the mechanism of the potassium carbonate catalysed gasification of activated carbon: The influence of the catalyst concentration on the reactivity and selectivity at low steam pressures. *Carbon* **1983**, *21*, 1–12. [[CrossRef](#)]

8. Radovic, L.R.; Walker, P.L., Jr.; Jenkins, R.G. Catalytic coal gasification: Use of calcium versus potassium. *Fuel* **1984**, *63*, 1028–1030. [[CrossRef](#)]
9. Kopyscinski, J.; Habibi, R.; Mims, C.A.; Hill, J.M. K_2CO_3 -Catalyzed CO_2 gasification of ash-free coal: Kinetic study. *Energy Fuels* **2013**, *27*, 4875–4883. [[CrossRef](#)]
10. Ciambelli, P.; Palma, V.; Russo, P.; Vaccaro, S. Redox properties of a TiO_2 supported Cu-V-K-Cl catalyst in low temperature soot oxidation. *J. Mol. Catal. A* **2003**, *204–205*, 673–681. [[CrossRef](#)]
11. Ciambelli, P.; D'Amore, M.; Palma, V.; Vaccaro, S. Catalytic oxidation of an amorphous carbon black. *Comb. Flame* **1994**, *99*, 413–421. [[CrossRef](#)]
12. Aneggi, E.; Leitenburg, C.; Dolcetti, G.; Trovarelli, A. Diesel soot combustion activity of ceria promoted with alkali metals. *Catal. Today* **2008**, *136*, 3–10. [[CrossRef](#)]
13. Weng, D.; Li, J.; Wu, X.; Si, Z.J. Modification of CeO_2 - ZrO_2 catalyst by potassium for NO_x -assisted soot oxidation. *Environ. Sci.* **2011**, *23*, 145–150. [[CrossRef](#)]
14. Castoldi, L.; Matarrese, R.; Lietti, L.; Forzatti, P. Intrinsic reactivity of alkaline and alkaline-earth metal oxide catalysts for oxidation of soot. *Appl. Catal. B* **2009**, *90*, 278–285. [[CrossRef](#)]
15. Lamallem, M.; Cousin, R.; Thomas, R.; Siffert, S.; Aissi, F.; Aboukaïs, A. Investigation of the effect of support thermal treatment on gold-based catalysts' activity towards propene total oxidation. *C. R. Chim.* **2009**, *12*, 772–778. [[CrossRef](#)]
16. Lakshmanan, P.; Delannoy, L.; Richard, V.; Méthivier, C.; Potvin, C.; Louis, C. Total oxidation of propene over $Au/xCeO_2-Al_2O_3$ catalysts: Influence of the CeO_2 loading and the activation treatment. *Appl. Catal. B* **2010**, *96*, 117–125. [[CrossRef](#)]
17. Gluhoi, A.C.; Bogdanchikova, N.; Nieuwenhuys, B.E. The effect of different types of additives on the catalytic activity of Au/Al_2O_3 in propene total oxidation: Transition metal oxides and ceria. *J. Catal.* **2005**, *229*, 154–162. [[CrossRef](#)]
18. Ali, A.M.; Daous, M.A.; Arafat, A.; AlZahrani, A.A.; Alhamed, Y.; Tuerdimaimaiti, A.; Petrov, L.A. Effect of Au Precursor and Support on the Catalytic Activity of the Nano-Au-Catalysts for Propane Complete Oxidation. *J. Nanomat.* **2015**, *2015*, 901439. [[CrossRef](#)]
19. Bozo, C.; Gaillard, F.; Guilhaume, N. Characterisation of ceria–zirconia solid solutions after hydrothermal ageing. *Appl. Catal. A* **2001**, *220*, 69–77. [[CrossRef](#)]
20. Liotta, L.F.; Di Carlo, G.; Pantaleo, G.; Venezia, A.M. Supported gold catalyst for CO oxidation and preferential oxidation of CO in H_2 stream: Support effect. *Catal. Today* **2010**, *158*, 56–62. [[CrossRef](#)]
21. Fu, Q.; Flytzani-Stephanopoulos, M. Active Nonmetallic Au and Pt Species on Ceria-Based Water-Gas Shift Catalysts. *Science* **2003**, *301*, 935–938. [[CrossRef](#)] [[PubMed](#)]
22. Eun Duck Park, E.D.; Lee, J.S. Effects of Pretreatment Conditions on CO Oxidation over Supported Au Catalysts. *J. Catal.* **1999**, *186*, 1–11. [[CrossRef](#)]
23. Venezia, A.M.; Pantaleo, G.; Longo, A.; Di Carlo, G.; Casaletto, M.P.; Liotta, L.F.; Deganello, G. Relationship between Structure and CO Oxidation Activity of Ceria-Supported Gold Catalysts. *J. Phys. Chem. B* **2005**, *109*, 2821–2827. [[CrossRef](#)] [[PubMed](#)]
24. Liotta, L.F.; Macaluso, A.; Longo, A.; Pantaleo, G.; Martorana, A.; Deganello, G. Effects of redox treatments on the structural composition of a ceria–zirconia oxide for application in the three-way catalysis. *Appl. Catal. A* **2003**, *240*, 295–307. [[CrossRef](#)]
25. Liotta, L.F.; Pantaleo, G.; Macaluso, A.; Marci, G.; Gialanella, S.; Deganello, G. Ceria-Zirconia Nanostructured Materials for Catalytic Applications: Textural Characteristics and Redox Properties. *J. Sol-Gel Sci. Tech.* **2003**, *28*, 119–132. [[CrossRef](#)]
26. Fonseca, A.A.; Fisher, J.M.; Ozkaya, D. Ceria-zirconia supported Au as highly active low temperature. Water-gas shift catalysts. *Top Catal.* **2007**, *44*, 223–235.
27. Liotta, L.F.; Longo, A.; Macaluso, A.; Martorana, A.; Pantaleo, G.; Venezia, A.M.; Deganello, G. Influence of the SMSI effect on the catalytic activity of a $Pt(1\%)/Ce_{0.6}Zr_{0.4}O_2$ catalyst: SAXS, XRD, XPS and TPR investigations. *Appl. Catal. B* **2004**, *48*, 133–149.
28. Wang, Q.; Zhao, B.; Li, G.; Zhou, R. Application of rare earth modified Zr-based ceria-zirconia solid solution in three-way catalyst for automotive emission control. *Environ. Sci. Technol.* **2010**, *44*, 3870–3875. [[CrossRef](#)]
29. Bekheet, M.F.; Grünbacher, M.; Schlicker, L.; Gili, A.; Doran, A.; Epping, J.D.; Gurlo, A.; Klötzer, B.; Penner, S. On the structural stability of crystalline ceria phases in undoped and acceptor-doped ceria materials under in situ reduction conditions. *CrystEngComm* **2019**, *21*, 145–154. [[CrossRef](#)] [[PubMed](#)]

30. Martorana, A.; Deganello, G.; Longo, A.; Deganello, F.; Liotta, L.; Macaluso, A.; Pantaleo, G.; Balerna, A.; Meneghini, C.; Mobilio, S. Time-resolved X-ray powder diffraction on a three-way catalyst at the GILDA beamline. *J. Synchrotron Rad.* **2003**, *10*, 177–182. [[CrossRef](#)] [[PubMed](#)]
31. Reveles, J.U.; Saoud, K.M.; El-Shall, M.S. Water inhibits CO oxidation on gold cations in the gas phase. Structures and binding energies of the sequential addition of CO, H₂O, O₂, and N₂ onto Au. *Phys. Chem. Chem. Phys.* **2016**, *18*, 28606–28616. [[PubMed](#)]



© 2020 by the authors. Licensee MDPI, Basel, Switzerland. This article is an open access article distributed under the terms and conditions of the Creative Commons Attribution (CC BY) license (<http://creativecommons.org/licenses/by/4.0/>).